Available online www.ejaet.com

European Journal of Advances in Engineering and Technology, 2023, 10(8):1-14

Research Article ISSN: 2394 - 658X

Microstructure and Dry Sliding Wear Behavior of Al-Zn-Mg Alloy Produced by Equal Channel Angular Pressing (ECAP)

Oryina Mbaadega Injor[1], Benjamin Omotayo Adewuyi[2], Oluyemi Ojo Daramola[3], Emmanuel Rotimi Sadiku[4], David Terfa Gundu[5], Sebastine Aondover Bam[6] and Julius Ngusha Akaaza[7]

[1, 5, 6, 7]Department of Mechanical Engineering, Joseph Sarwuan Tarka University, Makurdi.
[2, 3]Department of Metallurgical and Materials Engineering, The Federal University of Technology, Akure. Nigeria.
[4]Department of Chemical, Metallurgical and Materials Engineering, Tshwane University of Technology, Pretoria. South Africa.
*injorman@yahoo.com

ABSTRACT

An Al-Zn-Mg alloy locally produced by stir casting was subjected to equal channel angular pressing (ECAP) process at 200 ºC temperature. Microstructure, mechanical properties and wear behavior of the severely deformed Al-Zn-Mg alloy by ECAP process were studied. Microhardness and tensile strength tests were performed to evaluate the mechanical properties of the alloy. In addition, the wear tests were performed by using the ball on disc type test setup according to ASTM G-99 standard under 5 N normal load. The scanning electron microscope (SEM), was used to analyze the microstructure of specimens as well as the surface and debris of worn specimens. Mechanical properties results showed that the hardness and strength of the ECAP-processed alloy were higher than that of the as cast alloy and increased as the number of passes increases. The wear test data revealed that the wear rate and friction coefficient decreased with increasing ECAP passes. The SEM analysis of worn specimens demonstrated that the dominant wear mechanisms of the as cast alloy were adhesion wear and delamination, and the dominant wear mechanisms of ECAP processed alloy was abrasive wear. Oxidative wear was also observed at both as cast and ECAP processed alloy. Totally, these results demonstrated that ultrafine-grained structure fabricated by ECAP, improves the wear resistance of the Al-Zn-Mg alloy.

Key words: Al-Zn-Mg alloy; Equal channel angular pressing; Mechanical properties; Wear properties; Wear mechanism.

INTRODUCTION

Al-Zn-Mg alloy have been used as high strength, corrosion and wear resistance for industrial use because of their high strength to density ratio. Nowadays, there is much concern to enhance the mechanical behavior of Al-Zn-Mg alloy due to their widespread applications in aircraft, marine and transport industries [1-3]. In practice, several advanced engineering applications require a significantly complex combination of mechanical and tribological properties. Presently, the primary method to enhance the mechanical properties of the alloys is to change the material composition. However, this method has its own drawback and cannot considerably enhance the tribological properties of the alloys. It is essential to find a new technique to enhance the mechanical properties and wear resistance of the alloys. An effective technique to improve mechanical properties is to produce alumimium alloys with ultrafine-grained (UFG) microstructure using severe plastic deformation (SPD) processes [4, 5]. According to investigations, the SPD processes are reliable methods to attain the ultrafine grained microstructure [4]. These UFG microstructure materials with the high strength are in conformity with

the Hall-Petch relationship [6, 7]. Recently, equal channel angular pressing (ECAP) has been proven to be suitable for producing ultrafine-grained bulk materials. The technique also has the simplest design setup, with a noticeable strain achieved by repetitive pressing and can be applied to samples with varying types such as rods, bars and plates. [8-12]. During ECAP, a rod-shaped sample is pressed through an angular die with uniform cross section but bent in an L-shaped configuration. The material is subjected to large plastic shear deformation when forced to change in direction by 90º (intersection angel between two channels). Grain refinement occurs as a result of the large plastic shear deformation developed when the sample is forced through the L-shaped configuration of the die resulting in the spectacular enhancement of the strength of a working material [13]. Effective research attempts have been made recently, and successful presentations have been reported for several materials such as copper [14, 15], aluminium bronze alloys and Ti alloys [16], etc. The wear resistance is one of the most substantial properties of aluminum alloys with regards to the strength to density ratio and thermal conductivity. The distribution of hard second particles in aluminum alloys is done so as to improve the low wear resistance in aluminium [17]. A limited number of researches on the wear properties using SPD of materials showed that techniques such as ECAP leads to an enhancement in wear properties due to the improvement of mechanical properties. However, the effect of ECAP process on wear properties of the Al-Zn-Mg alloy was not investigated previously in details, therefore the tribological properties of the ECAP process on Al-Zn-Mg alloy were investigated in the present research. The dry sliding wear test was performed with the ball on disc type test setup according to ASTM G-99 standard. The wear test was conducted at 5 N load and 1 m/s sliding speed with a sliding distance of 282.09 m at 120 mm diameter track. Also, hardness and tensile strength of the alloy were measured. The wear mechanisms, surface and wear debris of the samples have also been determined using the scanning electron microscope (SEM).

EXPERIMENTAL PROCEDURES

Cast samples of Al-Zn-Mg alloy with rectangular shape and dimension (20×20×280) mm^3 were turned and machined to produce the required samples with dimension (15×15×90) mm^3 for ECAP pressing [18]. The chemical composition of the cast alloy (in wt %) was obtained using Atomic Absorption Spectrometry (AAS) as shown in Table 1.

The construction of the ECAP die was done locally from a split rectangular thick-walled steel with dimension (100×100×200) mm^3. An L-shaped channel of the same configuration was made on one of the split parts with dimension (15×15×230) mm^3 using AJAX 1 milling machine to give the pressing chamber. The ECAP die had an internal angle (Φ) of 90° and an additional angle of 20° at the outer radius of concordance (Ψ) where the two channels meet [19, 20].

The schematic diagram of ECAP die designed for pressing of aluminium and other light alloy samples is shown in fig. 1.

The heating of die and samples to a temperature of 200 °C was done using heating elements incorporated to the die, while a thermocouple enclosed in the die situated very close to the channel's intersection controlled the temperature. A punch was machined with dimension (14×14×250) mm^3 for pressing of samples into the channel under high pressure. The machined samples were initially preheated to a temperature of 500 ℃ and kept constant at that temperature for $\frac{1}{2}$ hrs in order to relieve stress using temperature control of resistance digital electric furnace with Model NYC 20.

After preheating, the samples were lubricated with molybdenum-based lubricant (Filtex) and loaded into the ECAP-Die with the ram inserted and the loading of the sample was completed, ready for pressing. The pressing was done using ELE Compact-1500 hydraulic compression testing machine at 2 mm/s using standard route Bc, in which the sample was rotated 90° clockwise around their longitudinal axis between consecutive passes [20-22]. This route was chosen in order to achieve equiaxed grains with increased fraction of high angle grain boundaries [23, 24].

A total of 32 samples were pressed using 200 ℃ temperature condition while 4 samples were used as control and not subjected to ECAP. Samples were identified by letter P followed by a digit indicating the ECAP pass number. Microstructure of samples after ECAP process was carried by optical microscopy (OM) and scanning electron microscopy (SEM). Samples for OM and SEM were prepared typically by metallographic preparation. Optical microscope model- Olympus DP72 with computerized imaging system was used to view the samples at 50 μm magnifications. Scanning electron microscopy (SEM) examinations were carried out on a Zeiss 540 ultra scanning microscope equipped with energy-dispersive spectrometer (EDS), and average grain size was calculated using linear intercept method.

X-ray diffractometer (XRD) with model- RAYONS X was used to examine the various phases present in the Al-Zn-Mg alloy. This was done using D/max- 250 x-ray diffractometer with Cu-Kα radiation of 1.54 Å at 30 kV

tube voltage and a current of 20 mA with a scanning speed of 1°/min. The crystal structures and their peak intensities were detected using X'Pert Highscore Plus software.

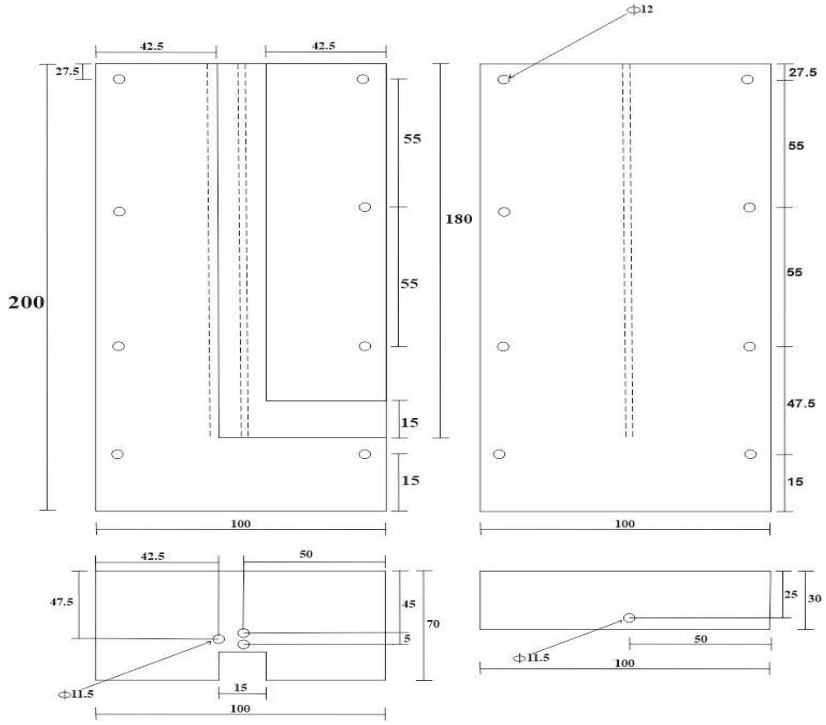

Fig 1: Schematic Diagram of the ECAP Die

Vickers method was used to determine the microhardness of specimen with dimensions $15\ mm \times 15\ mm$ according to ASTM E-834 using microhardness tester with model FM-800 where the applied load of 50 gm for 15 seconds dwell time was imposed on samples. Four measurements were taken from each sample and the average value was recorded. Tensile strength testing of all specimens was conducted using ASTME 8 standard. Tensile samples with dimensions of 50 mm gauge length, 12.5 mm width and 12.5 mm thickness were machined using EXCEL 14402 model lathe machine. Four identical tests specimen per sample were tested at room temperature with a strain/ loading rate of 5 mm/min using a computerized Instron Testing Machine with model- 3369. Four samples were tested at 200 ℃ and load displacement plots were obtained and ultimate tensile strength and yield strength values were also obtained from the machine.

Dry sliding wear test experiments were carried out by using ball on disc type test setup according to ASTM G-99 standard. The wear tests were carried out at 20 ºC temperature and at a relative humidity of 50 ± 5%. Samples for the wear test were machined into 20 mm length by 10 mm in breath and mounted on resin. The samples were made to slide against a 6 mm zirconia ball having hardness of 62 HRc and surface roughness 0.3 µm at a motor speed of 130 rpm. The wear test was conducted at 5 N load and 1 m/s sliding speed with a sliding distance of 282.09 m at 120 mm diameter track. The wear resistance was measured by weight loss method using a microbalance. The coefficient of friction ($\mu = F_f/P$) values were calculated by using frictional force data recorded in the computer and the applied load. Three samples were tested to confirm the repeatability of the results and the average values were taken into consideration.

Table -1. Chemical Composition of Al-Mg-Zn Alloy.

Element	Si	Fe	Cu	Mn	Mg	Cr	Ni	Zn	B	Be
Chemical Composition (%)	0.82	0.16	1.87	0.183	2.66	0.0194	0.102	5.79	0.0014	0.00046

Element	Bi	Ca	Co	Na	Pb	Sn	Zr	Al
Chemical Composition (%)	0.0035	0.0012	0.00061	0.00014	0.0505	0.0292	0.0029	88.2

RESULTS AND DISCUSSION

The microstructural images of samples of Al-Zn-Mg alloy produced before and after ECAP process at 200 ℃ is shown in Fig 2.

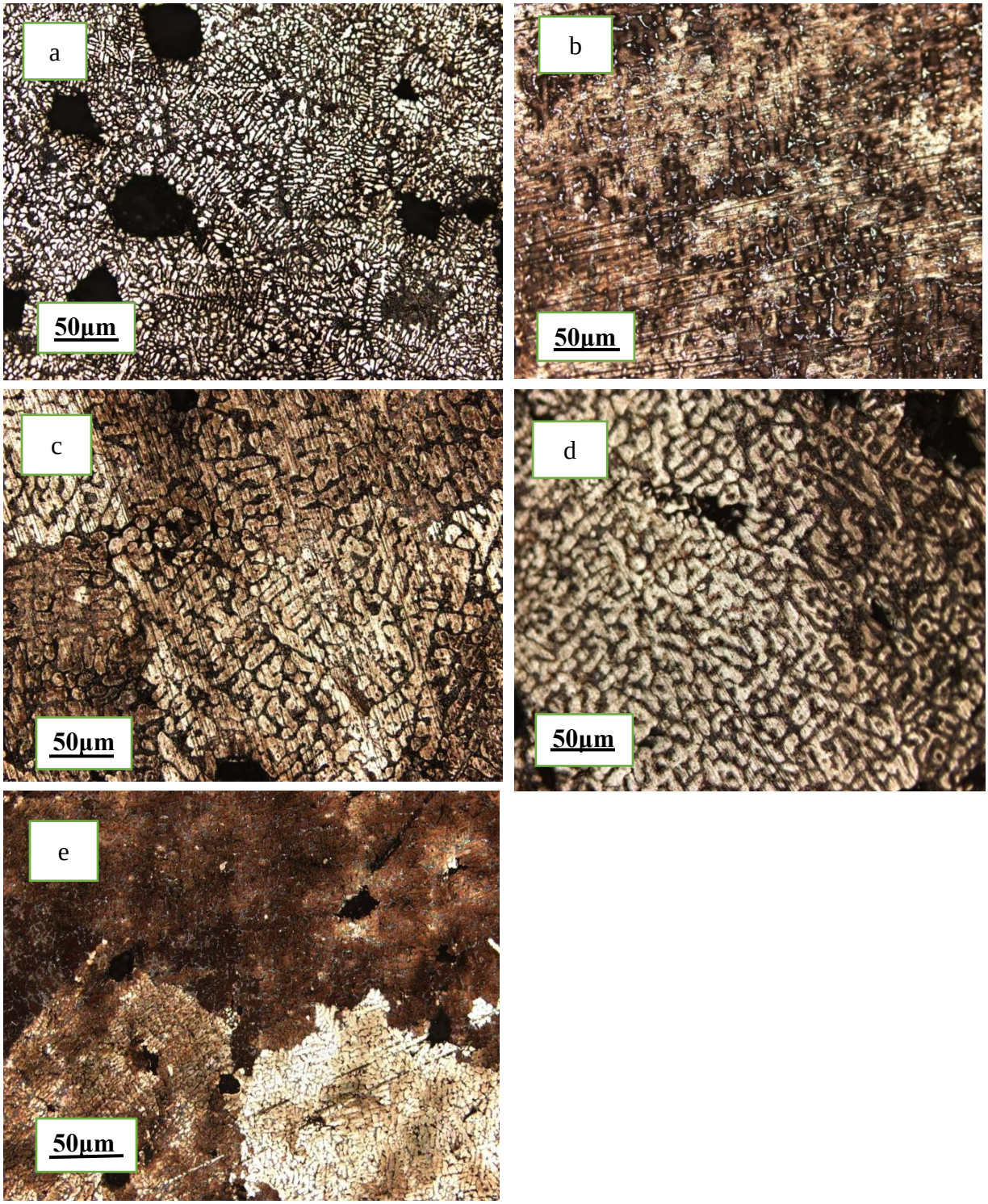

Fig 2: Optical Micrographs of Al-Zn-Mg Alloy; (a) As Cast (b) $P_1$200 (c) $P_2$200 (d) $P_3$200 (e) $P_4$200

From the results, it was noted that there was no significant precipitation in the as cast samples with reduced grain width and deformation bands (Fig 2a). But when the process was carried out at 200 ºC, precipitation was intensified as a result of activation of additional slipping systems at higher temperature. With risen number of ECAP passes from $P_1$200 to $P_4$200, the deformation bands became more evenly distributed and the subsequent microstructure became more refined (Fig 2b-e). The microstructure transformed into a fine equiaxial grain structure, which may also be ascribed to different slip planes that are initiated with the rotation of the sample thereby producing potentials for grain refinement using route Bc [25-27].
Fig. 3 illustrates the SEM micrographs of Al-Zn-Mg alloy processed at 200 ºC temperature condition.

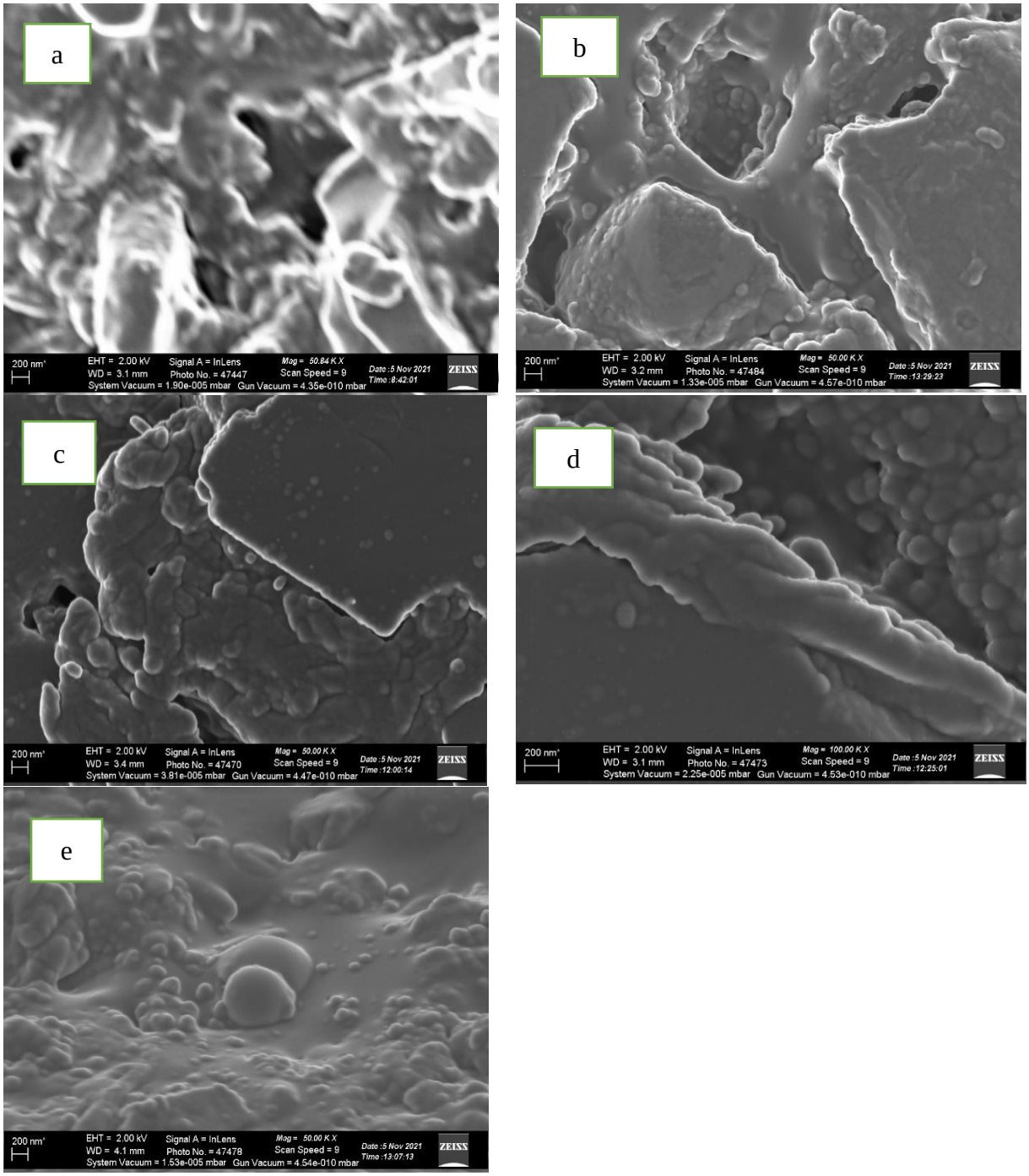

Fig 3: SEM Micrographs of Al-Zn-Mg Alloy for (a) As Cast (b) P_1200 (c) P_2200 (d) P_3200 (e) P_4200

The microstructure of the as-cast alloy reveals the distinctive feature of dendrites 250 ± 20 µm in size as shown in Figure 3a. In addition, η′ phase ($MgZn_2$) precipitates were noticed in the interdendritic regions (Zang *et al.*, 2010). The finer precipitations advance to pin the dislocations and grain boundaries which caused finer grain size and consequently increment of the mechanical properties. The grain structure was remarkably refined after P_1200 (Fig. 3b) with a grain size of 85 ± 15 µm. This is because of the development of sub-grain boundaries inside the grains with precipitate formed near the grain boundaries. In figure 3c a grain size of 50 ± 10 µm was observed in the microstructure of the alloy after P_2200. Figure 3d showed the development of shear bands inside the grains and sub-grains after P_3200 and these shear bands were 30 ± 8 µm in width. Figure 3e shows the microstructure of the alloy after P_4200, where shear bands were seen in this condition to be more with dimension of 10 ± 5 µm in width. Generally, the severe plastic deformation through ECAP process leads to refinement of $MgZn_2$ precipitations and subsequently decrement of the material flow in the wear direction which results in the improvement of wear properties [25].

X-ray diffractometry was used to ascertain the crystallographic structure of the alloy produced both before and after ECAP process for 200 ºC temperature condition as shown in Fig 4.

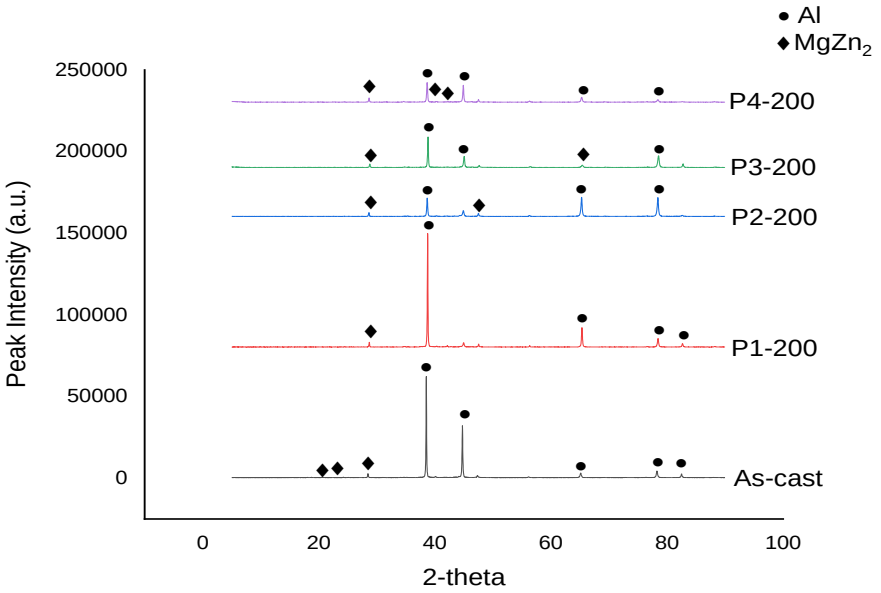

Fig 4: The X-ray Diffraction Patterns on the Cross-Sections of Samples after ECAP at 200 ºC Temperature Condition.

From the results it was found that there were peaks for aluminum and other phases in as-cast condition. The peaks at 20º tallies with Guinier–Preston (GP) zones while those at 40º–50º matches to intermetallic hexagonal η' ($MgZn_2$) phase and lastly lattice parameter of these peaks was marginally bigger than equilibrium η ($MgZn_2$) phase [28, 29]. GP zones are coherent with the aluminum matrix; metastable η' ($MgZn_2$) phase which is hexagonal in structure is semi-coherent with the aluminum matrix, while the equilibrium phase, η ($MgZn_2$), also hexagonal in structure is incoherent with the aluminum matrix [30].

Precipitates growth was seen in the alloy after P_1200, because of the space kept by dislocations for the growth of precipitates. As the number of ECAP passes increases, η' peaks moved towards the equilibrium η phase verifying the transformation of η' phase to stable η phase [28].

The shape of η' phase was formed in the initial phase of P_1200, and after increased number of ECAP passes, dislocation was developed as a result of shearing of this phase and consequently leading to the transformation of small-size spherical shape η phase ($MgZn_2$) [31]. This effect is attributed to the high dislocation density that acts as nucleation sites for more stable phases, due the faster diffusion of elements within the core of dislocations and by the larger space for the alloying atoms in the zones around these defects [25, 31].

Fig. 5 has shown the dependence of the microhardness on ECAP pass number of processed specimens. Generally, ECAP process caused an accentuated increase in the alloy microhardness. As can be seen, by increasing the pass number, the microhardness of the specimens increases notably.

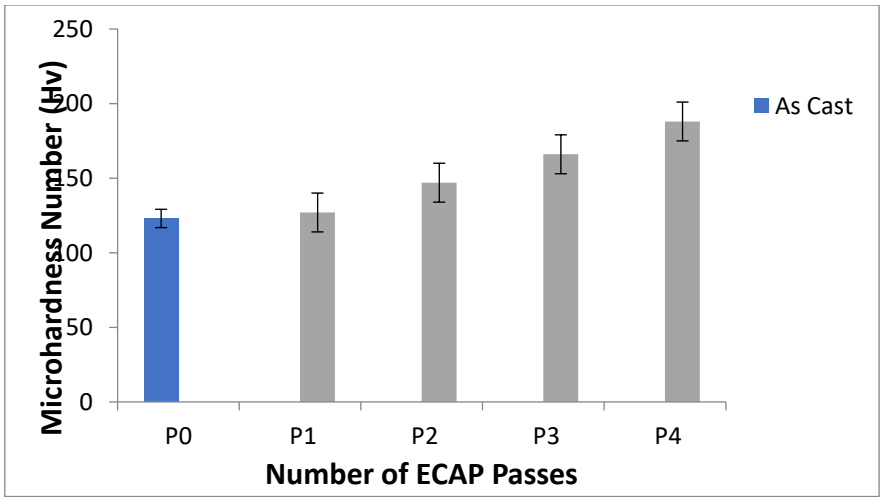

Fig 5: Plot of Microhardness against the Number of ECAP Passes

For P_0, the microhardness was 123 Hv, and thereafter there was notable improvement in the microhardness after ECAP processing. The microhardness of the alloy was improved to 127 Hv for P_1200, 147 Hv for P_2200, 166 Hv for P_3200 and 188 Hv for P_4200 respectively.

This increase in hardness, at 200 ºC ECAP processing temperatures results from precipitation, work hardening and microstructure refinement because of high dislocation density formed during ECAP processing and also the development of fine and elongated grain structure with deformation bands present in some grains interior that was distributed homogenously in the alloy [28]. Deformation bands are formed because it is not difficult for a constrained grain to deform by splitting into bands [27, 32]. This new high angle grain boundary formation induced by deformation can occur if there is increase in the misorientation between the deformation bands [25, 28]. On the other hand, according to Archard's law, the total volume of wear debris formed during wear test and subsequently wear rate is inversely proportional to the hardness [28]. So, by increasing the hardness of the alloy caused by grain refinement during ECAP process, the wear rate decreases.

The effect of Al-Zn-Mg alloy produced by ECAP technique on tensile and yield strength for 200 ºC temperature condition is shown in Fig 6.

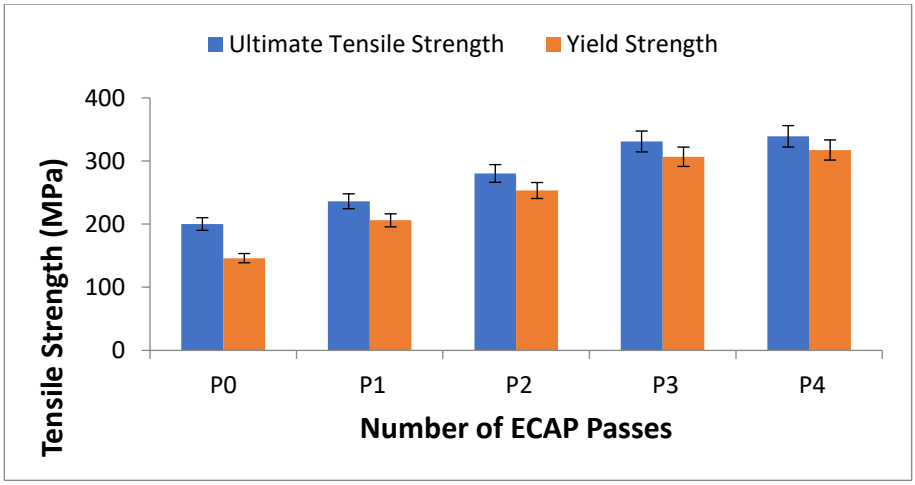

Fig 6: Plot of Tensile and Yield Strength against the Number of ECAP Passes.

It was observed that the Ultimate tensile strength (UTS) and the yield strength (YS) of Al-Zn-Mg alloy at 200 ºC increased with increase in the number of ECAP passes. For P_0, the UTS of the alloy was 200.22 MPa with a yield strength of 146.12 MPa. ECAP processing leads to a radical improvement in the strength of the material. After ECAP processing at 200 ºC, the UTS of the alloy increased from 236.18 MPa for P_1200, 280.26 MPa for P_2200, 330.96 MPa for P_3200 and 339.12 MPa for P_4200 respectively with corresponding increase in the yield strength from 146.12 MPa for P_1200 to 317.47 MPa for P_4200. The increase in yield strength is attributed to increase in dislocation density, work hardening and grain refinement during ECAP process described by Hall-Petch equation which states that the yield strength is inversely related to the average grain size of the material [28, 33].

The effect of Al-Zn-Mg alloy produced by ECAP technique on wear resistance for 200 ºC temperature condition is shown in Fig. 7.

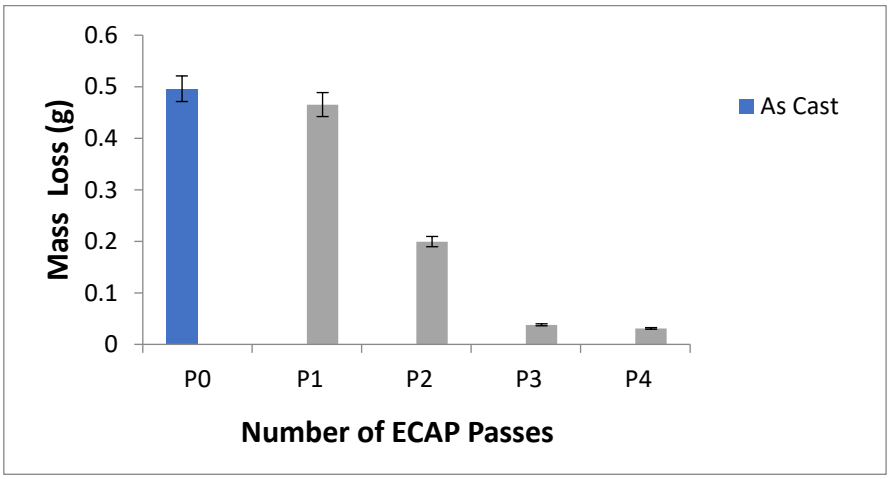

Fig 7: Plot of Mass Loss against the Number of ECAP Passes.

It was observed that, for the same load and the sliding speed, ECAP processed samples exhibits higher wear resistance than the as cast sample. The wear resistance of the alloy increased with increase in the number of passes at 200 ºC temperature condition. The mass loss also gradually reduced from 0.4654 g for the first pass to 0.0310 g after the fourth pass. In the as cast condition, the mass loss was 0.4961g which was the highest compared to 200 ºC temperature conditions. The improvement in the wear resisting capability of the material after ECAP processing is consistent with the earlier observations [34].

The effect of decrease in wear rate with hardness can be explained according to Archard's law [6] shown in Eq. 1.

$$Q = \frac{KLN}{H} \qquad (1)$$

where Q is volumetric wear loss, which is inversely proportional to the hardness H of the wear surface, L is the total sliding distance, N is the applied load and K is friction the coefficient. Consequently, the improvement in hardness of the alloy was achieved by grains and crystal refinement, thus improved hardness increases wear resistance of the alloy [35].

With the decrease of grain size after ECAP process, the hardness of the Al-Zn-Mg alloy also increases, and the wear volume decreases. This is because the hardness through ECAP process can improve the deformation resistance of the alloy. Furthermore, the volume fraction of second phase increases and the distribution of second phase rearranges after ECAP process, which strengthen the surface of the alloy. As a result, the wear resistance of the alloy improves remarkably after ECAP process.

The effect of Al-Zn-Mg alloy produced by ECAP technique on wear rate for 200 ºC temperature conditions is shown in Fig 8.

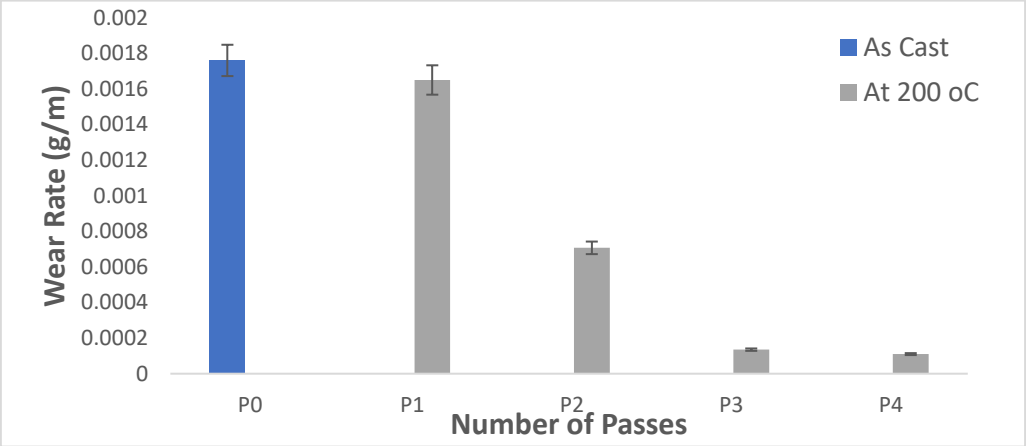

Fig 8: Plot of Wear Rate against the Number of ECAP Passes.

It was observed that the wear rate for the as cast sample was 0.0018g/m which is higher than those obtained for ECAP processed samples. The wear rate of the alloy decreased with increase in the number of passes for 200 ºC temperature conditions. There was a decrease in wear rate from 0.00165 g/m for the first pass to 0.0001099 g/m after the fourth pass. It is also obvious that the wear resistance is enhanced by increasing the number of passes [36]. This means that the grain size of the sample decreases with the wear rate [37].

The effect of Al-Zn-Mg alloy produced by ECAP technique on friction coefficient at 200 ºC temperature condition is shown in Fig 9.

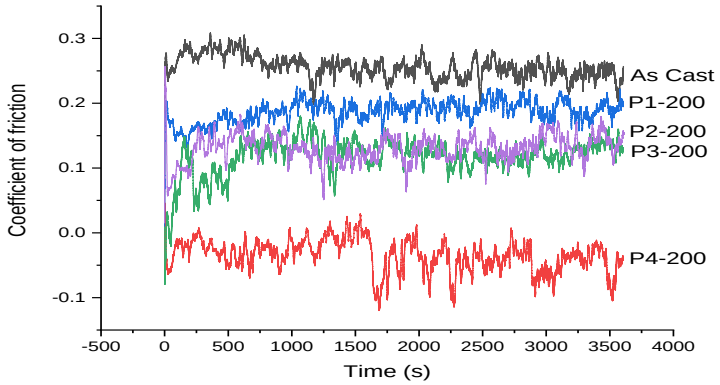

Fig 9: Plot of Coefficient of Friction against Time for Number of ECAP Passes.

It was observed that the coefficient of friction of the alloy in as cast condition was 0.27, which is higher than those obtained for ECAP processed samples. The coefficient of friction later decreased with increase in the number of ECAP passes for 200 ºC temperature condition. The coefficient of friction decreased from 0.19 for the first ECAP pass to -0.04 after the fourth ECAP pass.

Generally, there is decrease in the coefficient of friction with increase in ECAP passes for samples processed at 200 ºC temperature condition. This is because of the dependence of coefficient of friction of materials on mechanical properties (strength and hardness) as well as wear system [38].

The friction coefficient is related to adhesive wear and abrasive wear and can be expressed as shown in Eq. 2.

$$f = \frac{\tau_b}{\sigma_s} + \frac{2}{\pi} ctg\theta \qquad (2)$$

where τ_b is the shear strength and σ_s is the yield strength of the alloy. The first part of Eq. 2 is mainly caused by adhesive wear and the second part is decided by abrasive wear. After ECAP process, the yield strength of the alloy increases with increase in the number of passes. As a result of grain refinement after ECAP process, the size of abrasive particles decreases and are detached from the Al-Zn-Mg alloy which causes friction coefficient to decreases [39].

SEM images of the worn surface of the as-cast and ECAP processed samples under 200 ºC temperature condition at an applied load of 5 N is shown in Fig 10. It is found that the worn surface of the as-cast sample consists of adhesive, delamination and oxidation regions. There exists adhesion wear and plastic deformation along the direction of the sliding which results in delamination and oxide layer formation which shows that the wear mechanisms in the as-cast sample were adhesive, oxidative and delamination.

There were little scratches on the worn surface of the as-cast sample because of its lower hardness which showed the effect of abrasive wear. During the process of delamination, the material was separated from the ball surface and adhered to the steel disc [36]. Furthermore, the plastic deformation of surfaces in samples processed by ECAP becomes less intensive leading to decrease in adhesion wear and delamination. After four ECAP passes, the plowing bands in form of plastic deformation was seen and adhesion wear was relatively replaced by abrasive wear. Therefore, the dominant wear mechanism in the four ECAP pass samples was abrasive wear and as a result of the ECAP process, the amount of the adhesive wear was reduced compared to the as-cast sample.

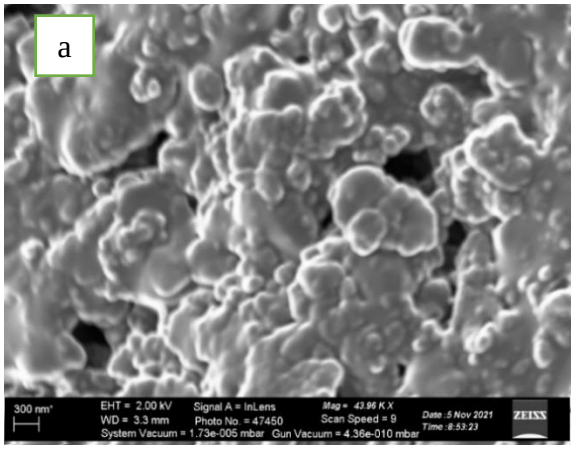

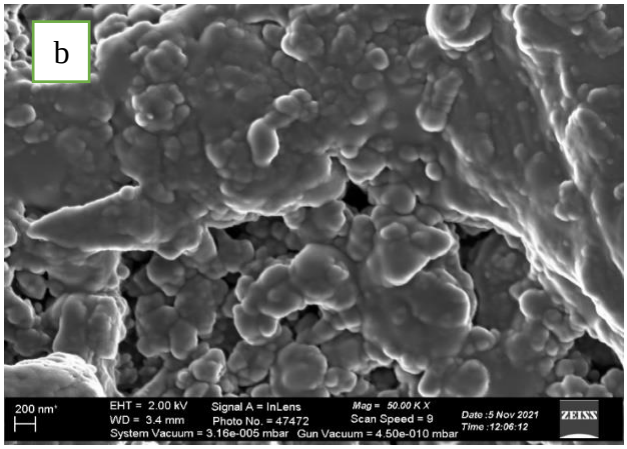

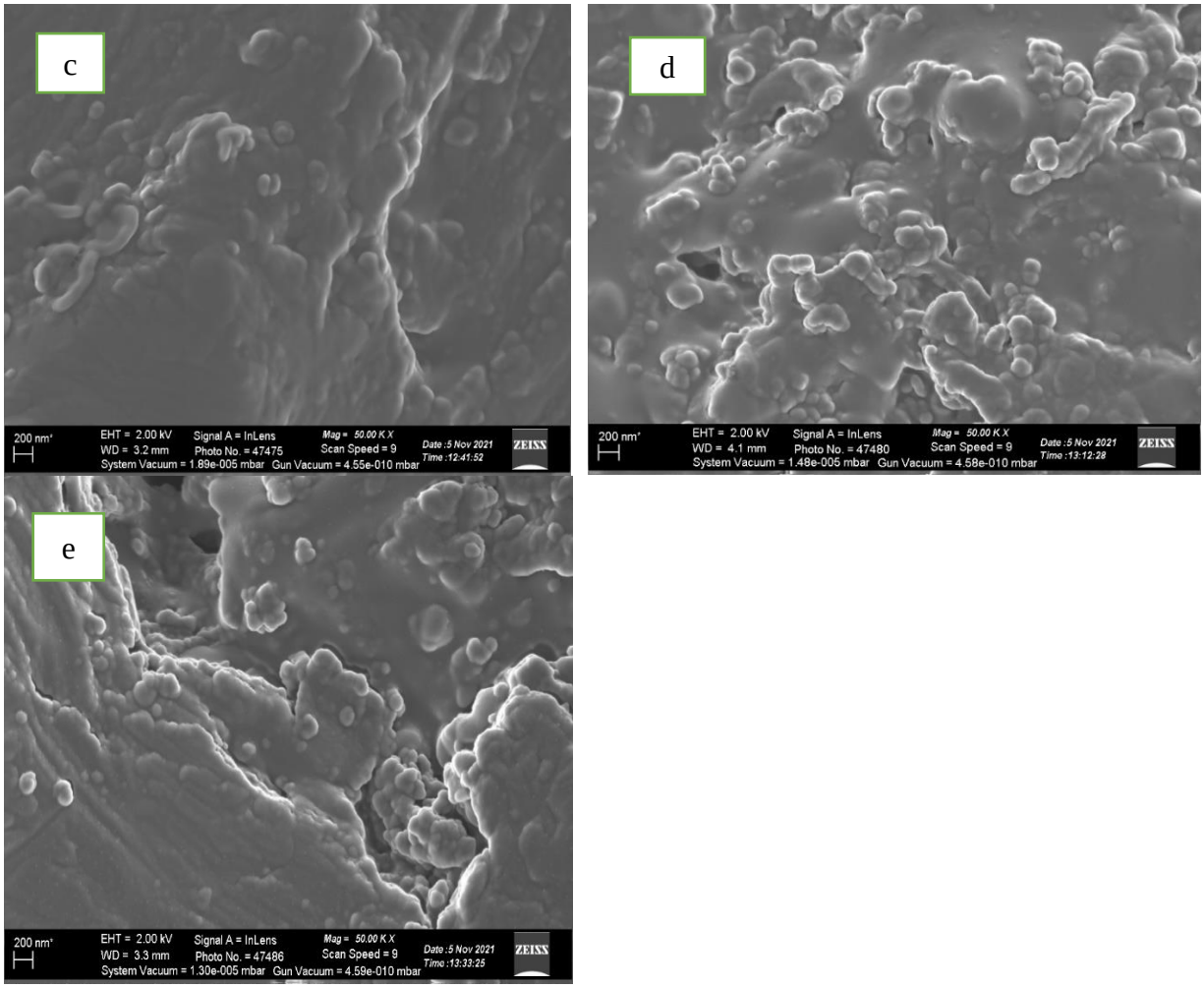

Fig 10: SEM Image of the Worn Surface of Al-Zn-Mg Alloy for; (a) Po (b) $P_1200\ ^0C$ (c) $P_2200\ ^0C$ (d) $P_3200\ ^0C$ (e) $P_4200\ ^0C$

Fig 11 showed SEM images of the wear debris of Al-Zn-Mg alloy collected during sliding under the applied load of 5 N for the as-cast and ECAP processed samples from one to four passes under 200 ^oC temperature condition. It can be observed that the size of the debris in ECAP samples are smaller than that of as-cast sample. The wear debris generated in wear test of as-cast sample was made up of two morphologies namely large plate-like and fine equiaxed morphologies. The presence of plate-like debris in the as-cast sample showed that delamination of the tribolayer occurred during sliding wear. As the strength and hardness increase during ECAP process, the plate-like morphology was transformed to fine equiaxed morphology indicating that the increased strength and hardness during ECAP process are the main reasons for the change in morphology of wear debris [40, 41].

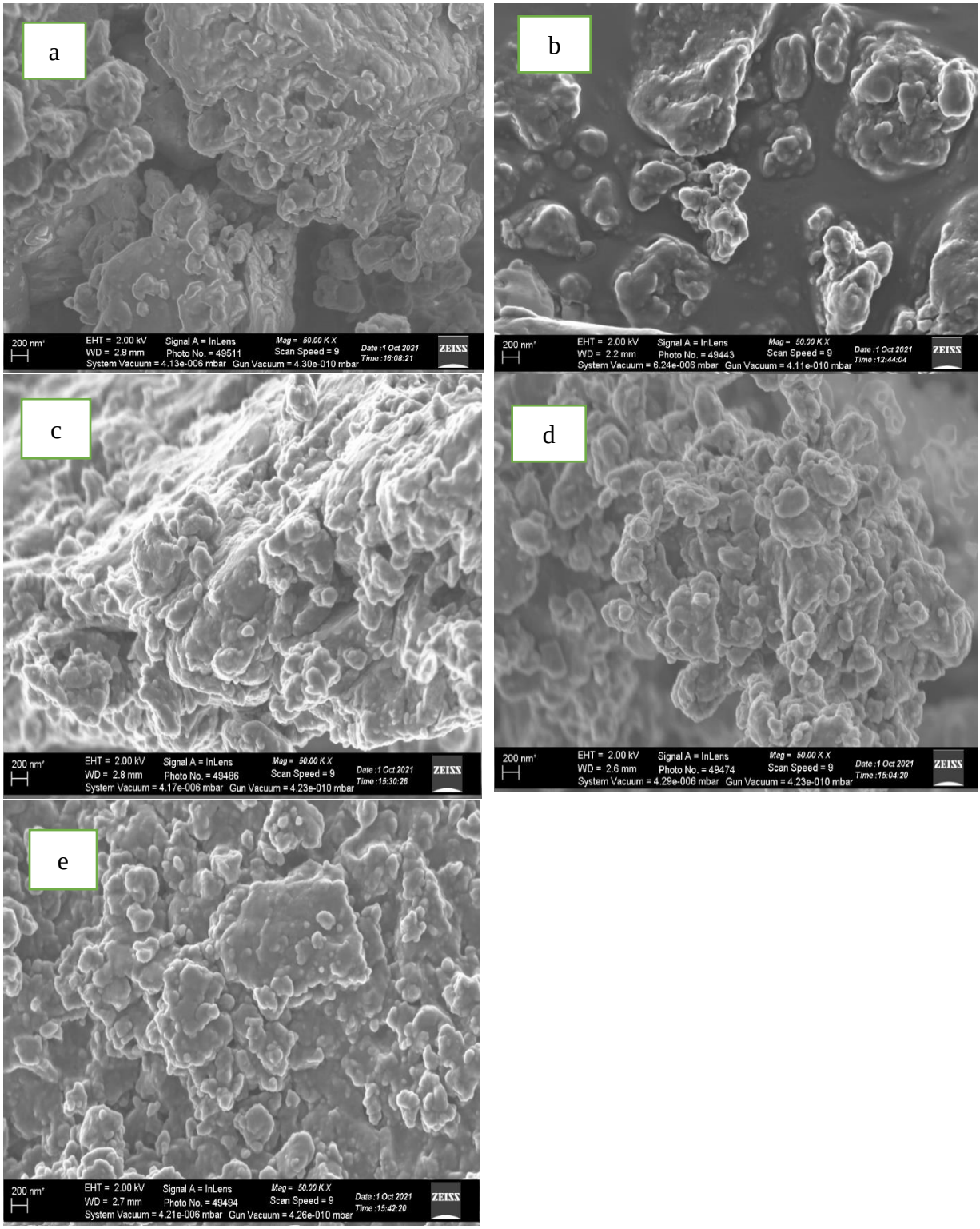

Fig 11: SEM Image of the Wear Debris of Al-Zn-Mg Alloy for; (a) Po (b) $P_1200\ ^0C$ (c) $P_2200\ ^0C$ (d) $P_3200\ ^0C$ (e) $P_4200\ ^0C$

CONCLUSION

Al-Zn-Mg Alloy produced locally was successfully deformed using equal channel angular pressing (ECAP) at a temperature of 200 ^{0}C.

Optical micrographs showed equiaxed and homogeneous microstructure in the third and fourth passes. There was no tangible precipitation in the as cast samples but precipitation was promoted at 200 ℃ because of activation of more slipping systems at higher temperatures.

SEM images of the as-cast alloy (P_0) exhibits dendrites of 250 ± 20 μm in size with η′ phase ($MgZn_2$) precipitates in the inter-dendritic regions, while there is significant refinement as the number of passes increased with sub-grain development within the boundary with precipitates developed near the grain boundaries for 200 ℃ ECAP temperatures. The grain refinement ranges from 85 ± 15 μm to 10 ± 5 μm for P_1200 to P_4200.

The XRD crystallographic structure showed peaks for aluminum and other phases in as cast condition with GP zones at 20^0 peaks and intermetallic hexagonal η' phase at $40^o - 50^o$ peaks. As the number of ECAP passes increases η' peaks moved towards the equilibrium η phase confirming the transformation of η' phase to stable η phase.

The microhardness of the alloy increase with decrease in the grain size. For P_0, the microhardness was 123 Hv, thereafter there was notable improvement in the microhardness after ECAP processing. This increase in hardness, at 200 ℃ ECAP processing temperatures results from precipitation, work hardening and microstructure refinement due to high dislocation density developed during ECAP processing.

The ultimate tensile strength and yield strength of Al-Zn-Mg alloy increased with increase in the number of ECAP passes. The highest tensile strength was 339.12 MPa with 317.47 MPa yield strength after the fourth ECAP pass.

The wear resistance was higher in the ECAP processed samples than the as cast sample and consequently increased with increase in the number of passes. The mass loss also gradually reduced from 0.4654 g for the first pass to 0.0310 g after the fourth pass.

The wear rate for the as cast sample was 0.0018g/m which is higher than those obtained for ECAP processed samples, which consequently decreased with increase in the number of passes. The wear rate decreased from 0.00165 g/m for the first pass to 0.0001099 g/m after the fourth pass.

The coefficient of friction of the alloy in as cast condition was 0.46 and later decreased with increase in the number of ECAP passes. This is because of the dependence of coefficient of friction of materials on mechanical properties (strength and hardness) as well as wear.

SEM images of the worn surface of the as-cast sample consists of adhesive, delamination and oxidation regions, showing little scratches because of its lower hardness. After ECAP process, adhesion wear was relatively replaced by abrasive wear.

The presence of plate-like wear debris in the as-cast sample showed that delamination of the tribolayer occurred during sliding wear. As the strength and hardness increase during ECAP process, the plate-like morphology was transformed to fine equiaxed morphology indicating that the increased strength and hardness during ECAP process are the main reasons for the change in morphology of wear debris.

REFERENCES

[1] JI Rojas and D Crespo, Dynamic Microstructural Evolution of an Al–Zn–Mg–Cu alloy (7075) During Continuous Heating and the Influence on the Viscoelastic Response, *Materials Characterization,* **2017**, 134, 319-328.

[2] X Xu, Y Zhao, B Ma and M Zhang, Electropulsing Induced Evolution of Grain-Boundary Precipitates without Loss of Strength in the 7075 Al Alloy, *Materials Characterization*, **2015**, 105, 90-94.

[3] G Chen, J Li, Z Yin and G Xu, Improvement of Microstructure and Properties in Twin-Roll Casting 7075 Sheet by Lower Casting Speed and Compound Field, *Materials Characterization*, **2017**, 127, 325-332.

[4] AP Zhilyaev, I Shakhova, A Belyakov, R Kaibyshev and TG Langdon, Wear Resistance and Electroconductivity in Copper Processed by Severe Plastic Deformation, *Wear*, **2013**, 305, 89-99.

[5] M Moghaddam, A Zarei-Hanzaki, M Pishbin, A Shafieizad and V Oliveira, Characterization of the Microstructure, Texture and Mechanical Properties of 7075 Aluminum Alloy in Early Stage of Severe Plastic Deformation, *Materials Characterization*, **2016**, 119, 137-147.

[6] L Gao and X Cheng, Microstructure and Dry Sliding Wear Behavior of Cu–10% Al–4% Fe Alloy Produced by Equal Channel Angular Extrusion, *Wear*, **2008**, 265, 986-991.

[7] C Cepeda-Jiménez, J García-Infanta, OA Ruano and F Carreño, Mechanical Properties at Room Temperature of an Al–Zn–Mg–Cu Alloy Processed by Equal Channel Angular Pressing, *Journal of Alloys and Compounds*, **2011**, 509, 8649-8656.

[8] C Xu and TG Langdon, The Development of Hardness Homogeneity in Aluminum and an Aluminum Alloy Processed by ECAP, *Journal of Materials Science*, **2007**, 42, 1542-1550.

[9] C Xu and TG Langdon, Influence of a Round Corner Die on Flow Homogeneity in ECA Pressing, *Scripta Materialia*, **2003**, 48, 1-4.

[10] RZ Valiev and TG Langdon, Principles of Equal-Channel Angular Pressing as a Processing Tool for Grain Refinement, *Progress in Materials Science*, **2006**, 51, 881-981.

[11] TG Langdon, The Principles of Grain Refinement in Equal-Channel Angular Pressing, *Materials Science and Engineering: A*, **2007**, 462, 3-11.

[12] SR Kumar, K Gudimetla, P Venkatachalam, B Ravisankar and K Jayasankar, Microstructural and Mechanical Properties of Al 7075 Alloy Processed by Equal Channel Angular Pressing, *Materials Science and Engineering: A*, **2012**, 533, 50-54.
[13] K-T Park, S-H Myung, DH Shin and CS Lee, Size and Distribution of Particles and Voids Pre-Existing in Equal Channel Angular Pressed 5083 Al Alloy: Their Effect on Cavitation During Low-Temperature Superplastic Deformation, *Materials Science and Engineering A*, **2004**, 371, 178–186.
[14] E Rabkin, I Gutman, M Kazakevich, E Buchman and D Gorni, Correlation Between the Nanomechanical Properties and Microstructure of Ultrafine-Grained Copper Produced by Equal Channel Angular Pressing, *Materials Science and Engineering A*, **2005**, 396, 11–21.
[15] WH Huang, L Chang, PW Kao and CP Chang, Effect of Die Angle on the Deformation Texture of Copper Processed by Equal Channel Angular Extrusion, *Materials Science and Engineering A*, **2001**, 307, 113–11
[16] ZH Li, GQ Xiang and XH Cheng, Effects of ECAE Process on Microstructure and Transformation Behavior of TiNi Shape Memory Alloy, *Materials and Design*, **2006**, 27, 324–328.
[17] B Venkataraman and G Sundararajan, Correlation Between the Characteristics of the Mechanically Mixed Layer and Wear Behaviour of Aluminium, Al-7075 Alloy and Al-MMCs, *Wear*, **2000**, 245, 22-38.
[18] C Xu, M Furukawa, Z Horita and TG Langdon, Using ECAP to achieve grain refinement, precipitate fragmentation and high strain rate superplasticity in a spray-cast aluminum alloy, *Acta Materialia*, **2003**, 51(20): 6139–6149.
[19] Y Iwahashi, J Wang, Z Horita, M Nemoto and TG Langdon, Principle of equal-channel angular pressing for the processing of ultrafine grained materials, *Scripta materialia*, **1996**, 35, 143-146.
[20] MH Shaeri, MT Salehi, SH Seyyedein, MR Abutalebi and JK Park, Characterization of Microstructure and Deformation Texture During Equal Channel Angular Pressing of Al–Zn–Mg–Cu Alloy, *Journal of Alloys and Compounds*, **2013**, 576, 350-357.
[21] M Shaeri, F Djavanroodi, M Sedighi, S Ahmadi, M Salehi and S Seyyedein, Effect of Copper Tube Casing on Strain Distribution and Mechanical Properties of Al-7075 Alloy Processed by Equal Channel Angular Pressing, *The Journal of Strain Analysis for Engineering Design*, **2013**, 48, 512-521.
[22] SM Masoudpanah and R Mahmudi, The Microstructure, Tensile, and Shear Deformation Behavior of an AZ31 Magnesium Alloy after Extrusion and Equal Channel Angular Pressing, *Materials and Design*, **2010**, 31, 3512-3517.
[23] K Oh-Ishi, Z Horita, M Nemoto, M Furukawa and TG Langdon, Optimizing the Rotation Conditions for Grain Refinement in Equal-Channel Angular Pressing, *Metallurgical and Materials Transactions A*, **1998**, 29, 2011-2013.
[24] Y Iwahashi, Z Horita, M Nemoto and TG Langdon, The Process of Grain Refinement in Equal-Channel Angular Pressing, *Acta Materialia*, **1998**, 46, 3317-3331.
[25] OM Injor, OO Daramola, BO Adewuyi, AA Adediran MM Ramakokovhu, ER Sadiku and ET Akinlabi, Grain Refinement of Al–Zn–Mg Alloy During Equal Channel Angular Pressing (ECAP), *Results in Engineering*, **2022**, 16, 1-9
[26] A Gholinia, PB Prangnell and MV Markushev, The Effect of Strain Path on The Development of Deformation Structures in Severely Deformed Aluminum Alloys Processed by ECAE, *Acta Materialia*, **2008**, 48, 1115–1130.
[27] PB Prangnell, JR Bowen and PJ Apps, Ultra-Fine Grain Structure in Aluminum Alloys by Severe Deformation Processing, *Materials Science and Engineering A*, **2004**, 375–377, 178–185.
[28] KR Cardoso, DN Travessa, WJ Botta and AM Jorge Jr, High Strength AA7050 Al Alloy Processed by ECAP: Microstructure and Mechanical Properties, *Materials Science and Engineering A*, **2011**, 528(18): 5804–5811.
[29] YH Zhao, XZ Liao, Z Jin, RZ Valiev and YT Zhu, Microstructures and Mechanical Properties of Ultrafine Grained 7075 Al Alloy Processed by ECAP and Their Evolutions During Annealing, *Acta Materialia*, **2004**, 52(15): 4589–4599.
[30] NQ Chinh, J Gubicza, T Czeppe, J Lendvai, C Xu, RZ Valiev and TG Langdon, Developing a Strategy for the Processing of Age Hardenable Alloys by ECAP at Room Temperature, *Materials Science and Engineering A*, **2009**, 516(1–2): 248–252.
[31] J Gubicza, I Schiller, NQ Chinh, J Illy, Z Horita and TG Langdon, The Effect of Severe Plastic Deformation on Precipitation in Supersaturated Al-Zn-Mg Alloys, *Materials Science and Engineering A*, **2007**, 460–461: 77–85.
[32] PJ Apps, JR Bowen and PB Prangnell, The Effect of Coarse Second-Phase Particles on the Rate of Grain Refinement During Severe Deformation Processing, *Acta Materialia*, **2003**, 51, 2811–2822.
[33] J Xing, H Soda, X Yang, H Miura and T Sakai, Ultra-Fine Grain Development in an AZ31 Magnesium Alloy During Multi-Directional Forging Under Decreasing Temperature Conditions, *Journal of Japan Institute of Light Metals*, **2005**, 46, 1646 – 1650.

[34] G Purcek, O Saray, T Kucukomeroglu, M Haouaoui and I Karaman, Effect of Equal-channel Angular Extrusion on the Mechanical and Tribological Properties of As-Cast Zn-40Al-2Cu-2Si Alloy, *Materials Science and Engineering A*, **2010**, 527(15), 3480– 3488.
[35] G Rahur, S Sanjay, KGV Preetham and KP Sanjay, Investigation of Mechanical Properties, Microstructure and Wear Rate of High Leaded Tin Bronze after Multidirectional Forging, *Procedia Materials Science*, **2014**, 5, 1081-1089.
[36] M Ebrahimi, S Attarilar, F Djavanroodi, C Gode and H Kim, Wear Properties of Brass Samples Subjected to Constrained Groove Pressing Process, *Materials and Design*, **2014**, 63, 531-537.
[37] E Ortiz-Cuellar, MAL Hernandez-Rodriguez and E García-Sanchez, Evaluation of the Tribological Properties of an Al–Mg–Si Alloy Processed by Severe Plastic Deformation, *Wear*, **2011**, 271 1828-1832.
[38] J Li, J Wongsa-Ngam, J Xu, D Shan, B Guo and TG Langdon, Wear Resistance of an Ultrafine-Grained Cu-Zr Alloy Processed by Equal Channel Angular Pressing, *Wear*, **2015**, 326, 10-19.
[39] SZ Wen, *Tribology*, Tinghua University Press, Beijing, **1990**.
[40] G Purcek, H Yanar, O Saray, I Karaman and H Maier, Effect of Precipitation on Mechanical and Wear Properties of Ultrafine-Grained Cu–Cr–Zr Alloy, *Wear*, **2014**, 311, 149-158.
[41] S Soleymani, A Abdollah-Zadeh and S Alidokht, Microstructural and Tribological Properties of Al5083 Based Surface Hybrid Composite Produced by Friction Stir Processing, *Wear*, **2012**, 278, 41-47.